

# Narrow gap Luttinger liquid in Carbon nanotubes

L. S. Levitov<sup>1</sup> and A. M. Tsvelik<sup>2</sup>

<sup>1</sup> *Department of Physics, Massachusetts Institute of Technology, 77 Massachusetts Ave., Cambridge MA02139*

<sup>2</sup> *Department of Physics, Brookhaven National Laboratory, Upton, NY 11973-5000*

(February 1, 2008)

Electron interactions reinforce minigaps induced in metallic nanotubes by an external field and turn the gap field dependence into a universal power law. An exactly solvable Gross-Neveu model with an  $SU(4)$  symmetry is derived for neutral excitations near half-filling. Charge excitations, described by a sin-Gordon perturbation of Luttinger liquid theory, are composite solitons formed by the charged and neutral fields with two separate length scales. Charge compressibility at finite density, evaluated in terms of inter-soliton interaction, exhibits a crossover from overlapping to non-overlapping soliton state. Implications for the Coulomb blockade measurements are discussed.

Electron interactions create a peculiar strongly correlated 1D electron system [1–5] in metallic Carbon nanotubes, the thinnest and the cleanest among the currently available nanoscale quantum wires. Luttinger liquid theory of nanotubes predicts [1,2] that, since tube diameter is larger than Carbon separation, the 1D electron coupling is mainly accounted for by the long-range electron interaction (forward scattering), while the exchange and Umklapp scattering, as well as backscattering, are relatively weak [5]. Recent experimental work [6–8] focused on Luttinger liquid effects in tunneling, observed as characteristic power laws in the tunneling current dependence on bias voltage and temperature.

Here we discuss Luttinger liquid effects in nanotubes with a minigap at the band center induced by an external perturbation. Such a minigap can be opened by parallel magnetic field [9] or by the intrinsic curvature of the tube [10]. The field- and curvature-induced gaps were observed experimentally [11,12] and found to be in agreement with the noninteracting electron model. We show that electron interaction enhances the charging gap and makes it a power law function of the bare gap.

This provides a unique situation, not available in other quantum wires, when Luttinger liquid effects are manifest in thermodynamical properties. For instance, in a gapped state induced by magnetic field, the bare gap is determined without any fitting parameters by Aharonov-Bohm flux through tube cross section, while the charging gap is directly measurable via Coulomb blockade, a prominent feature of transport in nanotubes [13–18]. In the strong forward scattering limit, the power law relation of the charging gap and magnetic field is characterized by a universal exponent  $4/5$ . We emphasize that the charging gap measurement is qualitatively different from the tunneling current measurement because it can be performed in thermodynamic equilibrium.

Also, in the presence of interactions the charging gap is much enhanced compared to the neutral excitation gap, while in a noninteracting system the two gaps are precisely equal. Large energy separation of the charged and neutral sectors results in high symmetry of the states in the neutral sector described by multiplets of

the group  $O(6) \sim SU(4)$  derived from exactly solvable Gross-Neveu model. This picture, demonstrated in the situation when the gapped state is created by external field, is realistic, since intrinsic interaction-induced gap in nanotubes are believed to be extremely small [19]

Electron bands of metallic tubes form two pairs of spin-degenerate right and left branches intersecting at the band center [20]. The Hamiltonian in the forward scattering approximation [1,2] has the form

$$\mathcal{H}_0 = -i\hbar v \int \sum_{j=1}^4 \psi_j^\dagger \sigma_3 \partial_x \psi_j dx + \frac{1}{2} \sum_q \rho_q V(q) \rho_{-q}, \quad (1)$$

where  $\psi_j(x)$  is a two component wavefunction,  $\rho(x) = \sum_{j=1}^4 \psi_j^\dagger(x) \psi_j(x)$  is charge density, and  $v$  is Fermi velocity. The form of the forward scattering amplitude in Eq.(1) depends on the electrostatic environment. In a nanotube of radius  $r$ , in the absence of screening,  $V(q) = \int V(x) e^{iqx} dx = e^2 \ln[(qr)^{-2} + 1]$ . The substrate dielectric constant  $\epsilon$  reduces  $V(q)$  by a factor  $2/(\epsilon + 1)$ .

Field-induced gapped state [9,10] is described by adding to the Hamiltonian (1) a backscattering term

$$\mathcal{V}_{\text{ext}} = \Delta_0 \int \sum_{j=1}^4 \psi_j^\dagger \sigma_1 \psi_j dx. \quad (2)$$

In the absence of interactions,  $V(q) = 0$ , electron spectrum is  $\epsilon(p) = \pm (v^2 p^2 + \Delta_0^2)^{1/2}$  with the value of  $\Delta_0$  depending on the backscattering mechanism. The magnetic field-induced gap [9] is linear in the field:  $\Delta_0 = \hbar v \phi / r$ , where  $\phi = \pi r^2 B / \Phi_0$  is the flux through tube cross-section scaled by  $\Phi_0 = hc/e$ . For typical tube radius  $r \simeq 0.5$  nm and  $B \simeq 10$  Tesla, the gap  $\Delta_0 \simeq 10$  meV.

We bosonize the Hamiltonian  $\mathcal{H} = \mathcal{H}_0 + \mathcal{V}_{\text{ext}}$  in the standard way, using  $\psi_j \propto e^{i\sqrt{\pi}\Phi_j}/r^{1/2}$ . The Gaussian part  $\mathcal{H}_0$  is diagonalized using linear combinations of the bosonic fields  $\Phi_j = (e_j^a \phi_a)$  with

$$\begin{aligned} \mathbf{e}_0 &= \frac{1}{2}(1, 1, 1, 1), & \mathbf{e}_1 &= \frac{1}{2}(1, -1, 1, -1), \\ \mathbf{e}_2 &= \frac{1}{2}(1, -1, -1, 1), & \mathbf{e}_3 &= \frac{1}{2}(1, 1, -1, -1) \end{aligned} \quad (3)$$

In this notation the Gaussian part of the Lagrangian describes one charged and three (neutral) flavor modes:

$$\mathcal{L}_0 = \frac{1}{2} \sum_q \{ \partial_\tau \phi_0(q) \partial_\tau \phi_0(-q) + K_q q^2 \phi_0(q) \phi_0(-q) \} + \frac{1}{2} \int dx \sum_{a=1}^3 (\partial_\mu \phi_a)^2, \quad K_q = 1 + \frac{4}{\pi} V(q) \quad (4)$$

( $\hbar = v = 1$ ). Bosonizing  $\mathcal{V}_{\text{ext}} = \Delta_0 \int dx \sum_{j=1}^4 (R_j^+ L_j + \text{h.c.})$ , we have

$$\mathcal{L}_\lambda = -2\lambda \int dx \left( \sum_{j=1}^4 \cos \sqrt{4\pi} \Phi_j \right) \quad (5)$$

with  $\lambda = \Delta_0/r$ . The total Lagrangian  $\mathcal{L} = \mathcal{L}_0 + \mathcal{L}_\lambda$  displays the fundamental  $U(1) \times SU(4)$  symmetry playing a major role in our analysis. Forward scattering makes the perturbation (5) even more relevant. At zero chemical potential the coupling  $\lambda$  grows under renormalization and opens spectral gaps.

There are several possible regimes in which a nanotube, described by Eqs.(4),(5), may exist. First, there is an insulating regime with the density at half-filling, where all excitations are gapped. Second, there are conducting states which can be realized by applying various external fields. These fields may close some gaps or even all of them, provided their magnitudes exceed certain critical values. For example, by varying chemical potential one can close all the gaps and make the perturbation  $\lambda$  irrelevant. This will lead to a transition into a metallic (Tomonaga-Luttinger liquid) regime. Fields breaking the  $SU(4)$  symmetry will not affect the charge sector and thus leave the system insulating, but may close some of the gaps in the flavor sector.

In a nanotube near half-filling, with no external fields present except  $\lambda$ , the perturbation (5) grows under RG as  $\lambda(l') = (l'/l)^{(1-\alpha)/4} \lambda(l)$ , where  $\alpha = K^{-1/2}$ . By the self-consistency argument  $\lambda(l') = 1/l'$ , the charge and flavor gaps are related to the noninteracting gap  $\Delta_0$  as

$$\Delta_{\text{fl}} \simeq \Delta_0 (D/\Delta_0)^{(1-\alpha)/(5-\alpha)}, \quad \Delta_{\text{ch}} \simeq K^{1/2} \Delta_{\text{fl}}, \quad (6)$$

where  $D = \hbar v/r$  is 1D bandwidth. Since  $\Delta_0$  is proportional to external magnetic field, Eq.(6) predicts a power law scaling of the gaps versus an experimentally controllable parameter. For high charge stiffness  $K_q \gg 1$ , the gap scaling exponent is universal, with the value  $4/5$ .

The separation (6) of the charge and flavor sector energy scales enables one to integrate out the fast mode  $\phi_0$  in adiabatic approximation. This will generate an effective action for the flavor modes with  $SU(4)$  symmetry. Separating  $\phi_0$  in the Lagrangian (5) one obtains

$$\mathcal{L}_\lambda = -4\lambda \int dx \left( u_1 \cos \tilde{\phi}_0 + u_2 \sin \tilde{\phi}_0 \right) \quad (7)$$

$$u_1 = \prod_{a=1}^3 \cos \tilde{\phi}_a, \quad u_2 = \prod_{a=1}^3 \sin \tilde{\phi}_a \quad (8)$$

where  $\tilde{\phi}_i = \sqrt{\pi} \phi_i$ . Treating the slow fields  $u_i$  as adiabatic parameters and shifting the variable

$$\phi_0 \rightarrow \phi_0 + \eta, \quad \eta = \pi^{-1/2} \tan^{-1}(u_2/u_1) \quad (9)$$

we transform the total Lagrangian  $\mathcal{L} = \mathcal{L}_0 + \mathcal{L}_\lambda$  as

$$\mathcal{L} = \mathcal{L}_0[\phi_0 + \eta] - \int dx M[\phi_a] \cos \tilde{\phi}_0 \quad (10)$$

with  $M[\phi_a] = 2\lambda \left( 1 + \sum_{a \neq b} \cos 2\tilde{\phi}_a \cos 2\tilde{\phi}_b \right)^{1/2}$ . From Eq.(10) we derive an effective action for the flavor sector valid for energies well below the charge gap (6) by integrating over the fast mode  $\phi_0$ . Let us examine the results of this integration. Writing the first term in (10) as  $\mathcal{L}_0[\phi_0] + \mathcal{L}_0[\eta] + \sum_{\omega, q} \{ \phi_0 \}_q (\omega^2 + K_q q^2) \{ \eta \}_q$  we note that the  $\eta$ -dependent terms are strongly irrelevant. For example,  $\mathcal{L}_0[\eta]$  contains squares of gradients

$$\partial_\mu \eta = \frac{\partial_\mu \phi_1 \sin 2\tilde{\phi}_2 \sin 2\tilde{\phi}_3 + \text{permut.}}{1 + \sum_{a \neq b} \cos 2\tilde{\phi}_a \cos 2\tilde{\phi}_b} \quad (11)$$

consisting of series of operators with the minimal scaling dimension 2. The relevant contribution arises from the last term of Eq.(10). Integrating it over  $\phi_0$  we obtain the ground state energy of the sine-Gordon model

$$-M^{2/(2-\alpha/4)}[\phi_a] = \text{const} - \lambda \sum_{a \neq b} \cos 2\tilde{\phi}_a \cos 2\tilde{\phi}_b + \dots = -g \sum_{a \neq b} : \cos 2\tilde{\phi}_a \cos 2\tilde{\phi}_b : + \dots \quad (12)$$

where  $g$  is a suitably renormalized coupling constant and dots stand for less relevant operators. The normal ordering is taken with respect to the new cut-off  $G$ .

Thus at energies smaller than the cut-off we obtain the effective action for the flavor modes in the form of the  $O(6) \sim SU(4)$  Gross-Neveu model:

$$\mathcal{L} = \int dx \left[ \frac{1}{2} \sum_{a=1}^3 (\partial_\mu \phi_a)^2 - g \sum_{a \neq b} : \cos 2\tilde{\phi}_a \cos 2\tilde{\phi}_b : \right] = \int dx [i \bar{\chi}_j \gamma_\mu \partial_\mu \chi_j - g : (\bar{\chi}_j \chi_j) (\bar{\chi}_k \chi_k) :] \quad (13)$$

where  $\chi_j$  ( $j = 1, \dots, 6$ ) are Majorana fermions. The latter model is exactly solvable, the spectrum consists of  $3 + 6 + 3$  relativistic particles with masses  $m, \sqrt{2}m, m$  transforming according to different representations of the  $O(6) \sim SU(4)$  group [21]. Their dispersion law is  $E_i(p) = (v^2 p^2 + m_i^2)^{1/2}$ . The Majorana fermions themselves belong to the vector representation of the group and carry mass  $\sqrt{2}m$ . The mass gap  $m$  depends on the bare parameters and can be crudely estimated as follows. The cut-off  $G$  is of order of the charge gap  $\Delta_{\text{ch}}$ ; it may be somewhat greater than  $\Delta_{\text{ch}}$  because the charge mode has a large velocity  $v_c = K^{1/2}v \gg v$  and therefore can be considered as fast in a larger region of the momentum space than for  $v_c = v$ . The value of the coupling constant  $g$  is such that the mass of the Gross-Neveu model (13) coincides with the physical spin gap (6):

$$G(\Delta_0) e^{-2\pi/3g} = \Delta_{\text{fl}} = f(K) \Delta_0 (D/\Delta_0)^{1/5} \quad (14)$$

At present we cannot estimate the function  $f(x)$ .

As for the charge excitations, they carry exactly the same quantum numbers as an electron. This happens because whenever a soliton of  $\phi_0$  is created, it acts as an effective potential for flavor fields forming bound states. The flavor fields coupled to a  $\phi_0$ -soliton give it the corresponding quantum numbers. Therefore, charge and flavor cannot be separated from each other in the charge sector.

In the sin-Gordon problem (4),(5) electron is represented by a soliton of one of the fields  $\Phi_j$ . Soliton spatial size can be estimated from a variational principle. Due to large charged stiffness  $K$ , the elastic energy of the soliton is dominated by the field  $\phi_0$ . According to (4) and (5), the soliton energy, estimated from the energy in the space interval  $l$  where the field  $\Phi_j(x)$  varies, is  $E(l) \simeq (K_{gl=1} l^{-2} + \lambda') l$  with renormalized coupling  $\lambda'(l) = \lambda(r/l)^{(3+\alpha)/4}$ . Soliton size  $w$  can be found by minimizing the energy with respect to  $l$ . Ignoring the logarithmic  $l$ -dependence of  $K$ , this gives  $w \approx (K/\lambda'(w))^{1/2}$ . The soliton energy  $E(w) \simeq (K\lambda'(w))^{1/2}$  coincides with the charge gap  $\Delta_{\text{ch}}$  in (6).

A peculiar feature of the composite charge soliton is the presence of two different length scales, because the flavor fields  $\phi_{1,2,3}$  vary faster than the more stiff charge field  $\phi_0$ . Let us consider a variational solution of the problem  $\mathcal{L}_0 + \mathcal{L}_\lambda$  with one of the fields  $\Phi_j$  varying between two minima of the energy (5). To be specific, we consider a soliton of the field  $\Phi_1 = \frac{1}{2}(\phi_0 + \dots + \phi_3)$  in which  $\Phi_1$  changes by  $\sqrt{\pi}$ , while  $\Phi_{1,2,3}$  do not change. In this case all fields  $\tilde{\phi}_0, \dots, \tilde{\phi}_3$  change by  $\pi/2$ . The length  $w$  over which the field  $\phi_0$  changes is much larger than that for  $\phi_{1,2,3}$ . Thus the variational problem for  $\tilde{\phi}_0$  can be treated in a  $\pi/2$  step approximation for  $\tilde{\phi}_{1,2,3}$ , as

$$\frac{1}{2} K (\tilde{\phi}_0')^2 = 4\pi\lambda' \left[ 1 - \max(\cos \tilde{\phi}_0, \sin \tilde{\phi}_0) \right] \quad (15)$$

(We treat  $K$  as a constant.) The solution of Eq.(15) with  $\tilde{\phi}_0 = \pi/4$  at  $x = 0$ , and the cos and sin terms contributing separately in the regions  $x > 0$ ,  $x < 0$ , is

$$\tilde{\phi}_0(x) = \begin{cases} 2 \cos^{-1} \tanh(u - x/w), & x < 0 \\ \frac{\pi}{2} - 2 \cos^{-1} \tanh(u + x/w), & x > 0 \end{cases} \quad (16)$$

where  $w = (K/4\pi\lambda')^{1/2} = \hbar v/\Delta_{\text{ch}}$ ,  $u = \tanh^{-1}(\cos \pi/8)$ .

The problem for the flavor fields is simplified because they vary in the region where  $\tilde{\phi}_0 \approx \pi/4$ . This gives

$$\frac{3}{2} \tilde{\phi}'^2 = 2^{3/2} \pi \lambda' (1 - \cos^3 \tilde{\phi} - \sin^3 \tilde{\phi}) \quad (17)$$

where  $\tilde{\phi} = \tilde{\phi}_{1,2,3}$ . Integrating Eq.(17) we obtain the function  $\tilde{\phi}(x)$ . As illustrated in Fig.1, the  $\tilde{\phi}_0$  step is  $\sim \sqrt{K}$  times wider than the  $\tilde{\phi}_{1,2,3}$  step. We emphasize that composite solitons in which all four fields  $\tilde{\phi}_i$  vary are charge excitations of the lowest possible energy.

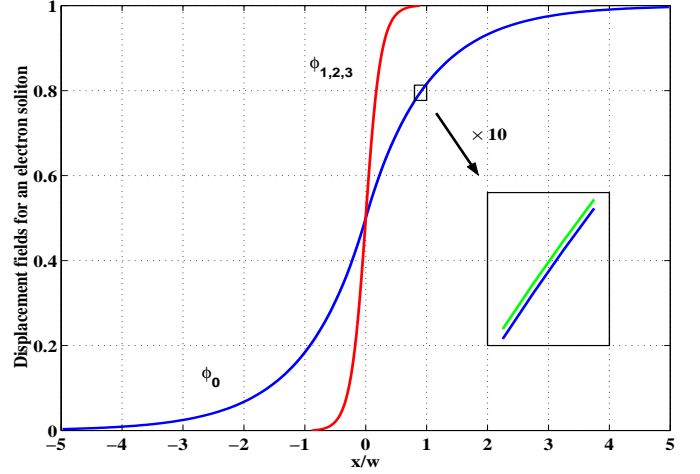


FIG. 1. Electron soliton charge and flavor parts [Eqs.(16),(17),(19)] scaled by  $\pi/2$ , with the stiffness  $K = 16$ . The scales for  $\tilde{\phi}_0(x)$  and  $\tilde{\phi}_{1,2,3}(x)$  differ by  $K^{1/2}$ . The approximate and exact solutions (19), (16) agree to 0.2%.

Now we consider multi-soliton solutions and determine charge compressibility from inter-soliton interaction. The compressibility  $\chi \equiv (d^2 E_n / d^2 n)^{-1}$ , with  $n$  the electron density, is directly related to the capacitance  $C = dn/dV_g$  and the charging spectrum measured in a Coulomb blockade experiment. The charging spectrum peak spacing is  $\delta_n = E_{n+1} - 2E_n + E_{n-1} \approx \chi^{-1}$ . We consider densities smaller than  $l_s^{-1}$  for which the charge fields  $\phi_0$  of different solitons may overlap, while the neutral cores with steps of  $\phi_{1,2,3}$  are isolated. The effective energy of the field  $\phi_0$  is obtained by minimizing (7) with respect to  $\tilde{\phi}_{1,2,3}$  at each value of  $\tilde{\phi}_0$ , which gives  $-4\lambda' \max_m \cos(\tilde{\phi}_0 + \frac{\pi}{2}m)$ . Switching between different branches occurs at  $\tilde{\phi}_0 = \frac{\pi}{4} + \frac{\pi}{2}m$ . Approximating cos by a parabola near each maximum one obtains

$$U(\tilde{\phi}_0) = 2\lambda' \min_m \left( \tilde{\phi}_0 - \pi m/2 \right)^2 \quad (18)$$

This approximation is extremely accurate, as illustrated in Fig.1 by comparing Eq.(16) with the soliton solution

$$\tilde{\phi}_0(x) = \begin{cases} \frac{\pi}{4} e^{x/w}, & x < 0 \\ \frac{\pi}{2} - \frac{\pi}{4} e^{-x/w}, & x > 0 \end{cases} \quad (19)$$

of the variational problem for the total energy

$$E[\tilde{\phi}_0] = \int dx \left( \frac{1}{2\pi} \partial_x \tilde{\phi}_0 \hat{K} \partial_x \tilde{\phi}_0 + U(\tilde{\phi}_0) \right) \quad (20)$$

with the interaction kernel  $\hat{K} = \delta(x - x') + \frac{4}{\pi} V(x - x')$ .

In a soliton lattice the field  $\tilde{\phi}_0(x)$  is a continuous monotonic function with smooth  $\pi/2$  steps, as in Fig.1. To evaluate the energy (20), we introduce a periodic *discontinuous* field  $\varphi = \tilde{\phi}_0 - \pi m/2$  with integer  $m$  chosen to minimize  $U(\tilde{\phi}_0)$ . The energy (20) with  $\tilde{\phi}_0 = \varphi - \frac{\pi}{2} \sum_m \theta(x - ma)$  takes the form

$$\int dx \left[ \frac{1}{2\pi} (\partial_x \varphi + \frac{\pi}{2} G(x)) \hat{K} (\partial_x \varphi + \frac{\pi}{2} G(x)) + 2\lambda' \varphi^2 \right] \quad (21)$$

where  $G(x) = \sum_m \delta(x - ma)$ . The advantage of the form (21) is that this *quadratic* function can be easily minimized in the Fourier representation. We obtain

$$\varphi(q) = -iq \frac{\pi}{2} G(q) K_q / (K_q q^2 + 4\pi\lambda') \quad (22)$$

with  $G(q) = 2\pi \sum_n \delta(qa - 2\pi n)$ . The energy of (22) is

$$E[\varphi] = \sum_q 4\lambda' K_q \left( \frac{\pi}{2} G(q) \right)^2 / (K_q q^2 + 4\pi\lambda') \quad (23)$$

Using the identity  $G^2(q) = L G(q)$ , with  $L$  the system size, the energy density can be written as

$$E(n) = \hbar v \frac{\pi n^2}{8} \sum_{m=-\infty}^{\infty} \frac{4\pi\lambda' K_{q_m}}{K_{q_m} q_m^2 + 4\pi\lambda'} \quad (24)$$

with  $q_m = 2\pi m/a$  and soliton density  $n = 1/a$ .

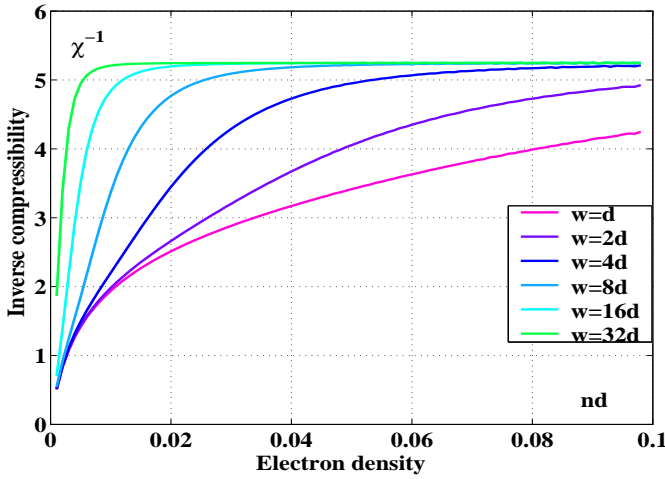


FIG. 2. Charge compressibility  $\chi = (d^2 E(n)/d^2 n)^{-1}$  scaled by  $1/\hbar v$  plotted for several soliton widths  $w = (4\pi\lambda')^{-1/2}$ . Eq.(25) was used with the screening length  $l_s = 0.2 \mu\text{m}$ ,  $v = 8 \cdot 10^7 \text{cm/s}$ ,  $\epsilon = 12$ , tube diameter  $d \equiv 2r = 1 \text{nm}$ .

Charge compressibility obtained from Eq.(24) with

$$K(q) = 1 + \frac{2}{\epsilon + 1} \frac{4e^2}{\pi \hbar v} \ln [(q^2 + r^{-2})/(q^2 + l_s^{-2})] \quad (25)$$

that models screening (e.g., by a gate) at distance  $l_s \gg r$  is plotted in Fig.2. At high density  $n \gg w^{-1}$ , compressibility is density-independent,  $\chi_0^{-1} = \frac{\pi}{4} \hbar v + \frac{4e^2}{\epsilon + 1} \ln(l_s/r)$ . At lower  $n \ll w^{-1}$  it varies as  $\chi^{-1} = \chi_0^{-1} - \frac{4e^2}{\epsilon + 1} \ln(rn)$ . The crossover can be explained by noting that neighboring overlapping solitons interact via  $V(r) \propto r$ , while non-overlapping solitons interaction is  $V(r) \propto 1/r$ , because

electric field is screened and confined to 1D at  $r \leq w$  and becomes deconfined at  $r \geq w$ .

The crossover density  $n \simeq w^{-1}$  is sensitive to the magnetic field which controls soliton size  $w = \hbar v / \Delta_{\text{ch}}$ . Thus the compressibility dependence on soliton size (Fig.2) is manifest in the charging spectrum dependence on magnetic field. Along with the power law field dependence (6) of the gap at half-filling, it represents novel 1D electron correlation phenomenon observable in a narrow gap state of nanotubes in thermodynamic equilibrium.

This work is supported by the MRSEC Program of the National Science Foundation under Grant No. DMR 98-08941 and by US DOE under contract No. DE-AC02-98CH10886.

- 
- [1] C. Kane, L. Balents, M. P. A. Fisher, Phys. Rev. Lett. **79**, 5086 (1997),
  - [2] R. Egger, A. O. Gogolin, Phys.Rev.Lett. **79**, 5082 (1997)
  - [3] L. Balents, M. P. A. Fisher, Phys. Rev. B **55**, R11973 (1997)
  - [4] Yu. A. Krotov, D.-H. Lee, and S. G. Louie, Phys. Rev. Lett. **78**, 4245 (1997)
  - [5] A. Odintsov, H. Yoshioka, Phys. Rev. Lett. **82**, 374 (1999)
  - [6] M. Bockrath, *et al.*, Nature **397**, 598 (1999)
  - [7] R. Egger, *et al.*, Luttinger liquid behavior in metallic carbon nanotubes, cond-mat/0008008
  - [8] A. Bachtold, *et al.*, Phys. Rev. Lett. **87**, 166801 (2001)
  - [9] H. Ajiki and T. Ando, J. Phys. Soc. Jpn. **62**, 1255 (1993); J. Phys. Soc. Jpn. **65**, 505 (1996).
  - [10] C. L. Kane, E. J. Mele, Phys. Rev. Lett. **78**, 1932 (1997).
  - [11] J. -O. Lee, *et al.*, Sol. Stat. Comm. **115**, 467 (2000).
  - [12] C. Zhou, J. Kong, and H. Dai, Phys. Rev. Lett. **84**, 5604 (2000).
  - [13] S. J. Tans, *et al.*, Nature, **386**, 474 (1997).
  - [14] M. Bockrath, *et al.*, Science **275**, 1922 (1997)
  - [15] S. J. Tans, *et al.*, Nature **394**, 761 (1998)
  - [16] D. H. Cobden, *et al.*, Phys. Rev. Lett. **81**, 681 (1998).
  - [17] J. Nygard, *et al.*, Nature, **408**, 342 (2000).
  - [18] W. Liang, M. Bockrath, H. Park, Phys. Rev. Lett. **88**, 126801 (1998).
  - [19] The leading interaction, forward scattering, does not open a gap, while other interactions are just marginally relevant in the renormalization group [1,2] and also small numerically [5].
  - [20] R. Saito, G. Dresselhaus, and M. S. Dresselhaus, *Physical Properties of Carbon Nanotubes* (Imperial College Press, London, 1998).
  - [21] A. B. Zamolodchikov and Al. B. Zamolodchikov. Ann. Phys. (NY) **120**, 253 (1979).